Proc. Natl. Acad. Sci. USA
Vol. 90, pp. 1078–1082, February 1993
Biochemistry

The unusual metal clusters of nitrogenase: Structural features revealed by x-ray anomalous diffraction studies of the MoFe protein from *Clostridium pasteurianum*

JEFFREY T. BOLIN*†, ALICIA E. RONCO*‡, T. VANCE MORGAN§, LEONARD E. MORTENSON§, AND NGUYEN-HUU XUONG¶

*Department of Biological Sciences, Purdue University, West Lafayette, IN 47907; §Center for Metalloenzyme Studies, Department of Biochemistry, University of Georgia, Athens, GA 30602; and ¶Departments of Physics, Chemistry and Biology, University of California, San Diego, La Jolla, CA 90923

Communicated by Michael G. Rossmann, August 19, 1992

ABSTRACT **Nitrogenase (EC 1.18.6.1) catalyzes the conversion of dinitrogen to ammonia, the central reaction of biological nitrogen fixation. X-ray anomalous diffraction data were analyzed to probe the structures of the metal clusters bound by nitrogenase MoFe protein. In addition to one FeMo cofactor, each half-molecule of MoFe protein binds one large FeS cluster of a type not previously observed in a protein. The FeS cluster contains roughly eight Fe atoms, comprises two subclusters, and is separated from the FeMo cofactor by an edge-to-edge distance of 14 Å. The inorganic framework of the FeMo cofactor is not resolved into subclusters, but the Mo atom is located at its periphery. FeMo cofactors in different half-molecules are 70 Å apart and cannot promote binuclear activation of dinitrogen by two Mo atoms.**

The six-electron reduction of dinitrogen to ammonia is the central reaction of biological nitrogen fixation and thus a key process in the global nitrogen cycle (1, 2). The catalyst for this reaction, nitrogenase (EC 1.18.6.1), is a remarkable multicomponent metalloenzyme complex. Although forms without Mo (3, 4) exist, the best-characterized nitrogenase is a Mo-dependent enzyme (5–7) comprising two easily separated metalloproteins. Component 1, an $\alpha_2\beta_2$ MoFe protein, M_r = 220,000–240,000, contains approximately 2 Mo, 30 Fe, and 30 inorganic S atoms arranged as unusual metal–sulfur clusters of undefined structure. Component 2, a homodimeric Fe protein, M_r = 60,000–70,000, binds a single Fe_4S_4 cluster as well as MgATP/MgADP (8). Both components are required for reduction of N_2 by a process which follows the limiting stoichiometry

$$8H^+ + 8e^- + N_2 \rightarrow 2NH_3 + H_2 \qquad [1]$$

and involves transfer of electrons from the Fe protein to the MoFe protein with concomitant hydrolysis by the two-protein complex of two MgATP molecules for each electron transferred.

The MoFe protein contains a unique prosthetic group known as the FeMo cofactor, or FeMoco (9), which is the likely site of substrate binding and reduction. The known components of FeMoco include 1 Mo, 6–7 Fe, 6–9 inorganic S atoms, and 1 molecule of homocitrate; two FeMocos bind per tetramer, accounting for the total Mo and half of the Fe content of MoFe protein. In spite of the fact that it has been extracted, purified, and extensively studied by a variety of techniques, the structure of FeMoco is not known and its properties have not been satisfactorily reproduced in model compounds (10, 11). The Fe atoms not associated with FeMoco also are collected into atypical clusters. In an earlier model for the structure of MoFe protein they were divided into four Fe_4S_4 clusters, called "P-clusters," which were assigned spectroscopic and redox properties that are both novel and complex (5–7). Thus it is likely that all of the metal atoms bound by MoFe protein are associated with metal–sulfur clusters of unusual structure and/or environment.

The basic features of the crystal structure of Fe protein have been described by Georgiadis *et al.* (12). Here we report multi-wavelength x-ray anomalous diffraction studies that provide further information about the structures of the metal–sulfur clusters bound by MoFe protein as well as their relative positions within the protein molecule.

METHODS

Theoretical Background. X-ray anomalous diffraction experiments exploit the influence of resonant x-ray absorption on x-ray scattering (13). This dependence is usually defined by equating the total atomic scattering factor, f, with the sum of a real wavelength-independent "normal" scattering factor, f°, and a complex wavelength-dependent "anomalous" scattering term, $f' + if''$. The anomalous scattering factors f' and f'' depend on atomic number as well as wavelength. Moreover, the wavelength dependence for a specific atom is especially strong in the vicinity of one of its x-ray absorption edges. Thus the anomalous scattering of particular atoms such as metals bound to a protein can be isolated through measurement of differences in reflection intensities. Our experiments exploit "Bijvoet differences," which depend on f'' and result from anomalous scattering caused by the K-shell absorption of the Mo, Fe, and S atoms present in MoFe protein.

The Bijvoet differences are expected to be small compared with the average structure factor amplitude. For Cu-Kα radiation, on the basis of the scattering factors listed in Table 1 and M_r = 220,000, we expect that the Bijvoet diffraction ratio (13)—i.e., the ratio of the average difference to the average amplitude—should be 3.1–8.8%; for Co-Kα radiation, the ratio should be 1.2–3.5%. In both cases, the lower limit was derived by assuming independent atoms (2 Mo, 30 Fe, and 32 S), whereas the upper limit was determined by treating the six clusters in the standard model as group scatterers. In fact, the ratio should approach the upper limit at zero scattering angle and decline to the lower limit as the angle increases to include reflections of spacings smaller than the diameters of the clusters (≈4–5 Å).

Anomalous Diffraction Measurements. Monoclinic crystals of MoFe protein from *Clostridium pasteurianum* were used

The publication costs of this article were defrayed in part by page charge payment. This article must therefore be hereby marked "*advertisement*" in accordance with 18 U.S.C. §1734 solely to indicate this fact.

Abbreviations: FeMoco, FeMo cofactor; MIR, multiple isomorphous replacement.

†To whom reprint requests should be addressed.
‡Present address: Centro de Investigaciones del Medio Ambiente, Facultad de Ciencias Exactas, Universidad Nacional de la Plata, 1900-La Plata, Argentina.

for these experiments. The crystals were grown and mounted in a glove box under N_2 atmosphere (14, 15). The space group is $P2_1$; the unit cell dimensions are: a = 69.9 Å, b = 151.2 Å, c = 121.8 Å, β = 110.2°; the asymmetric unit contains one MoFe protein tetramer.

Anomalous diffraction experiments were performed at the University of California at San Diego Multiwire Area Detector Facility (16), using Cu-Kα (λ = 1.54 Å) and Co-Kα (λ = 1.79 Å) radiation from a conventional x-ray generator. The use of these two wavelengths, which bracket the Fe-K absorption edge, makes it possible to exploit variations in the relative anomalous scattering of Fe and Mo as described below. The data collection strategy was specifically designed to measure Bijvoet differences and is similar to the strategy for monoclinic crystals described by Xuong *et al.* (17), except that paired 30° ω scans were used to measure reflections related by Friedel symmetry from the same crystal by 'inverse-beam' geometry; that is, one scan at χ_1 and ϕ_1 was followed by a scan over the same ω range but with $\chi_2 = -\chi_1$ and $\phi_2 = \phi_1 + 180°$.

In the case of the Cu-Kα data we measured 450,000 observations of 148,000 reflections (point group 2) extending to spacings of 2.6 Å with R_{sym} = 3.7%, where $R_{sym} = \{\Sigma_h\Sigma_i|I_{hi} - I_h|\}/\{\Sigma_h\Sigma_i I_{hi}\}$, sums over i span all symmetry-related observations of a reflection, sums over h span all independent reflections, I_{hi} is the scaled intensity of an observation, and I_h is the mean intensity. For the 5.0-Å subset, R_{sym} = 3.1%, and the average redundancy is 5 observations per independent reflection in point group 2. If the data are merged in point group 2/m (Bijvoets merged), R_{sym} = 5.0% for the 2.6- and 5.0-Å subsets. The Co-Kα data include 652,000 observations of 92,500 reflections extending to 3.0 Å with R_{sym} = 5.3%; for the 5.0-Å subset, R_{sym} = 4.8% and the average redundancy is 12 observations per reflection. If the data are merged in point group 2/m, R_{sym} = 5.8% for the 3.0-Å data and 5.4% for the 5.0-Å subset. Given R_{sym} as an estimate of the relative error in a single intensity measurement, an error statistic roughly comparable to the Bijvoet difference ratio is error of $(\Delta F/F) = R_{sym}/(2n)^{1/2}$, where ΔF is the difference between mean values of F^+ and F^- and n is the average redundancy. Based on the above, the relative error in the measurement of Bijvoet differences for reflections with spacings larger than 5.0 Å should be 1% for either wavelength.

RESULTS

Analysis of Bijvoet Difference Patterson Maps. A Cu-Kα Bijvoet difference Patterson map (18) was calculated, using reflections with spacings between 20 and 5 Å. Such a map should display peaks at positions corresponding to vectors between anomalous scatterers; for this resolution range the metal and sulfur atoms within a cluster are not resolved, and each cluster can be considered a single scatterer. Thus the asymmetric volume of the map should contain one peak for every unique pair of clusters in the unit cell of the crystal, and the relative positions of the clusters should be deducible from the set of intercluster vectors. Given two FeMocos and four P-clusters per tetramer, and two tetramers per unit cell, the expected result is 36 independent intercluster vectors, 6 of which give rise to peaks on the Harker plane, V = ½. These 6 result from pairs of clusters related by crystallographic symmetry, and we expect one Harker peak for each independent cluster in the tetramer: 2 arising from pairs of FeMocos and 4 arising from pairs of P-clusters.

Additional information may be derived from the peak amplitudes, since the magnitude of a peak relating clusters A and B should be roughly proportional to the product $\Sigma_A \times \Sigma_B$, where Σ_A and Σ_B are sums of the f'' values for the atoms in A and B. On the basis of the data in Table 1, $\Sigma f''$ for FeMoco ($MoFe_7S_8$: 30 e^-) is twice that for a P-cluster (Fe_4S_4: 15 e^-); hence the two Harker peaks that relate FeMocos should have 4 times the density of the four Harker peaks that relate P-clusters.

Table 1. Expected anomalous scattering contributions of various atoms and groups for Cu-Kα and Co-Kα radiation

	Cu-Kα (λ = 1.54 Å)		Co-Kα (λ = 1.79 Å)	
Scatterer	f', e^-	f'', e^-	f', e^-	f'', e^-
Atoms				
Mo	−0.2	2.7	−0.1	3.5
Fe	−1.2	3.2	−3.4	0.5
S	0.3	0.6	0.4	0.7
Groups				
$MoFe_7S_8$		30		13
Fe_4S_4		15		5
Fe_8S_8		30		9

The values of f' and f'' for atoms were calculated by using the program described by Cromer (19). Values of f'' for groups are sums of the atomic contributions.

The Harker section of a Cu-Kα Bijvoet difference Patterson map is shown in Fig. 1. Instead of two strong and four markedly weaker peaks, there are four peaks of roughly equivalent amplitude. Furthermore, elsewhere in the map we find exactly 12 additional peaks of similar amplitude rather than 30 additional peaks of various amplitudes. As shown in Table 2, the maximum values for all 16 peaks are within a factor of ±35% of the average maximum value of 74. Aside from the origin peak, these peaks account for all but one (section V = 0, maximum = 38) of the set with a maximum value larger than 35. The distribution of peaks is entirely consistent with the binding by MoFe protein of four metal-sulfur clusters, all of which contain approximately the same number of metal atoms. Hence, the Fe atoms not associated with FeMoco apparently are bound in two large and presumably identical clusters of a type that contains approximately 8 Fe atoms.

Because the energies of Cu-Kα and Co-Kα radiation lie on either side of, but close to, the Fe-K absorption edge, the use of Co-Kα radiation allows a distinction to be made between Harker peaks related to FeMocos and those related to the all-Fe clusters. While $\Sigma f''$ for a $MoFe_7S_8$ cluster is 13 e^-, that for a Fe_8S_8 cluster is only 9 e^-, and Harker peaks corresponding to vectors between FeMocos should be stronger by a factor of approximately 2.

The Harker section from a 20- to 5-Å Co-Kα Bijvoet difference Patterson map is shown adjacent to the corresponding section from the Cu-Kα map in Fig. 1. Two of the prominent peaks in the Cu-Kα section are represented by the

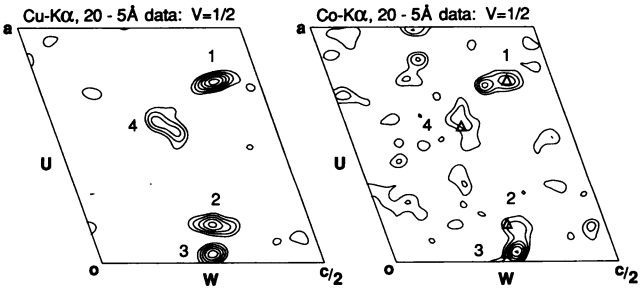

FIG. 1. Harker sections of Bijvoet difference Patterson maps based on Cu-Kα and Co-Kα anomalous diffraction data. Both maps were calculated by using reflections with spacings between 20 and 5 Å. In both cases, the first contour is at 20% of the maximum on the Harker section and the interval between contours is 15% of the maximum. The Δs plotted on the Co-Kα section mark the positions of the maxima of corresponding peaks in the Cu-Kα map. U, V, and W are the coordinates of the Patterson map.

Table 2. Peaks in a Cu-Kα Bijvoet difference Patterson map

Patterson peak, type	Between clusters	Relative height	Fractional coordinates		
			U	*V*	*W*
1, Harker	1 and 1′	100	0.764	0.500	0.391
2, Harker	2 and 2′	82	0.167	0.500	0.273
3, Harker	3 and 3′	87	0.042	0.500	0.250
4, Harker	4 and 4′	58	0.576	0.500	0.250
a, general	1 and 2	80	0.806	0.047	0.055
b, general	1 and 2′	73	0.958	0.453	0.328
c, general	1 and 3	67	0.639	0.172	0.430
d, general	1 and 3′	85	0.597	0.336	0.180
e, general	1 and 4	69	0.389	0.094	0.438
f, general	1 and 4′	84	0.847	0.398	0.180
g, general	2 and 3	57	0.556	0.219	0.500
h, general	2 and 3′	53	0.403	0.281	0.242
i, general	2 and 4	69	0.194	0.148	0.484
j, general	2 and 4′	68	0.639	0.352	0.234
k, general	3 and 4	94	0.236	0.062	0.000
l, general	3 and 4′	60	0.806	0.438	0.250

The 16 largest nonorigin peaks in the asymmetric unit of a map based on data with interplanar spacings between 20 and 5 Å are listed. Peak and cluster numbers correspond to the labels in Fig. 1. Primed numbers designate clusters related to the unique set by crystallographic symmetry.

strongest two features in the Co-Kα section, whereas the other two correspond to weaker peaks close to the noise level: the maximum densities in the vicinity of Cu-Kα peaks 1 and 3 are 52 and 74, respectively, whereas the highest values near peaks 2 and 4 are 36 and 35. We infer that peaks 1 and 3 arise from the FeMocos and peaks 2 and 4 arise from the all-Fe clusters.

Given this identification it was possible to determine the positions of the two FeMocos and two all-Fe clusters associated with a single MoFe protein molecule. The positions of the four unique clusters were first expanded by crystallographic symmetry into neighboring unit cells. The expanded set was then examined to identify groups that contain one copy of each of the four original clusters and meet additional criteria derived from the size and shape of MoFe protein (20, 21) as well as the direction of its twofold molecular symmetry axis (22). Specifically, groups contained within a sphere 90 Å in diameter such that the positions of nominally identical clusters are related by the molecular twofold symmetry axis were considered. These criteria identify a unique group of four clusters defined by the following crystallographic fractional coordinates, where the numbers correspond to the labels in Fig. 1: 1, FeMoco, (0.118, 0.000, 0.304); 2, all-Fe, (−0.084, −0.047, 0.364); 3, FeMoco, (0.479, 0.172, 0.875); 4, all-Fe, (0.712, 0.094, 0.875). These positions indicate that the two FeMocos are separated by 70 Å and the distance between the all-Fe clusters is 71 Å. Each FeMoco is paired with an all-Fe cluster (1 with 2, 3 with 4) separated by a center-to-center distance of 19 Å or an edge-to-edge distance of 14 Å. Both types of clusters lie on line segments that are perpendicular (within 2°) to the direction of the molecular twofold axis; thus each of the four clusters is roughly 35 Å from the axis. The distance between the line defined by the FeMocos and that defined by the all-Fe clusters is 9 Å. Additional evidence for this arrangement is provided by anomalous diffraction studies of a recently prepared crystalline form of *Azotobacter vinelandii* MoFe protein in that Cu-Kα Bijvoet difference Patterson maps based on data from these crystals are consistent with the arrangement of clusters described above for the clostridial enzyme (J.T.B. and S. W. Muchmore, unpublished data).

Analysis of Bijvoet Difference Electron Density Maps. Additional information on the structure of FeMoco and the all-Fe cluster was acquired by analysis of Bijvoet difference electron density maps (23). To obtain these maps, we assigned spherically symmetric scattering models to the clusters and calculated resolved-anomalous phases (24) on the basis of the Cu-Kα anomalous diffraction data and a partial structure comprising only the clusters. This initial phase set allowed facile interpretation of heavy-atom difference Fouriers for three Pt derivatives. Multiple isomorphous replacement (MIR) phases were then calculated and used to prepare Bijvoet difference electron density maps, which thus are unbiased with respect to the models assigned to the clusters.

In Fig. 2 we show Bijvoet difference electron density in the vicinity of one FeMoco and one all-Fe cluster from maps calculated by using 20- to 5-Å Cu-Kα or Co-Kα data. For the all-Fe cluster, the Cu-Kα density shows two partially resolved maxima separated by approximately 4.5 Å. Moreover, the shape of the density envelope is consistent with a tetrahedral arrangement of Fe atoms in both halves. A reasonable interpretation is that the all-Fe cluster consists of two subclusters similar to typical Fe_4S_4 or Fe_3S_4 clusters.

The FeMoco density in the Cu-Kα map includes roughly the same total volume as the all-Fe cluster, but at this resolution it shows no evidence of subclusters: there is only one central maximum and there is no indication of a "waist" at the boundary. However, comparison of the Cu-Kα and Co-Kα maps does provide information on the position of the Mo atom within the metal–sulfur framework of FeMoco. Inasmuch as the f'' values of Mo and Fe are nearly equivalent for Cu-Kα radiation, the boundary of the Cu-Kα density should be a good indication of the external shape of the framework. But because f'' of Mo is dominant for Co-Kα radiation, a maximum corresponding to the position of the Mo and its S ligands (25, 26) should be present in the Co-Kα map. Indeed, the Co-Kα map shows a strong maximum that is clearly offset from the center of the Cu-Kα density envelope but nevertheless contained within an overall feature of comparable shape and volume. Examination of digital maps indicates the Co-Kα maximum is 3–4 Å from the center of the Cu-Kα density but is not substantially closer (<1 Å) than is the center to the edge of the all-Fe cluster.

DISCUSSION

In the following discussion the above results are used to draw a number of conclusions with respect to the structure and function of MoFe protein, the properties of the clusters, and the interpretation of previous biochemical and biophysical experiments that probe these properties.

Our results show that MoFe protein binds four metal–sulfur clusters of approximately equivalent metal content: two FeMoco and two all-Fe clusters. They further show that the clusters occur in pairs such that each half-molecule contains one FeMoco and one all-Fe cluster, and that FeMocos in different half-molecules are separated by 70 Å. These results contradict those from a prior diffraction study of the *A. vinelandii* MoFe protein (27). That study, on the basis of low-resolution electron density maps phased by direct methods, suggested that the FeMocos are separated across the molecular twofold axis by approximately 20 Å center-to-center and 7 Å edge-to-edge. It was also suggested that a conformational change could reposition the FeMocos so that the two Mo atoms could jointly bind and activate a single dinitrogen molecule. Our evidence shows that this is impossible and that nitrogenase does not function by homobinuclear activation of dinitrogen by Mo.

The large separation (≈35 Å) of both FeMoco and the all-Fe cluster from the molecular twofold axis implies that either or both could be close to the surface of the protein. In fact, 4-Å electron density maps phased by a combination of anomalous diffraction and MIR methods (not shown) demonstrate that both are no farther than 10 to 15 Å from the

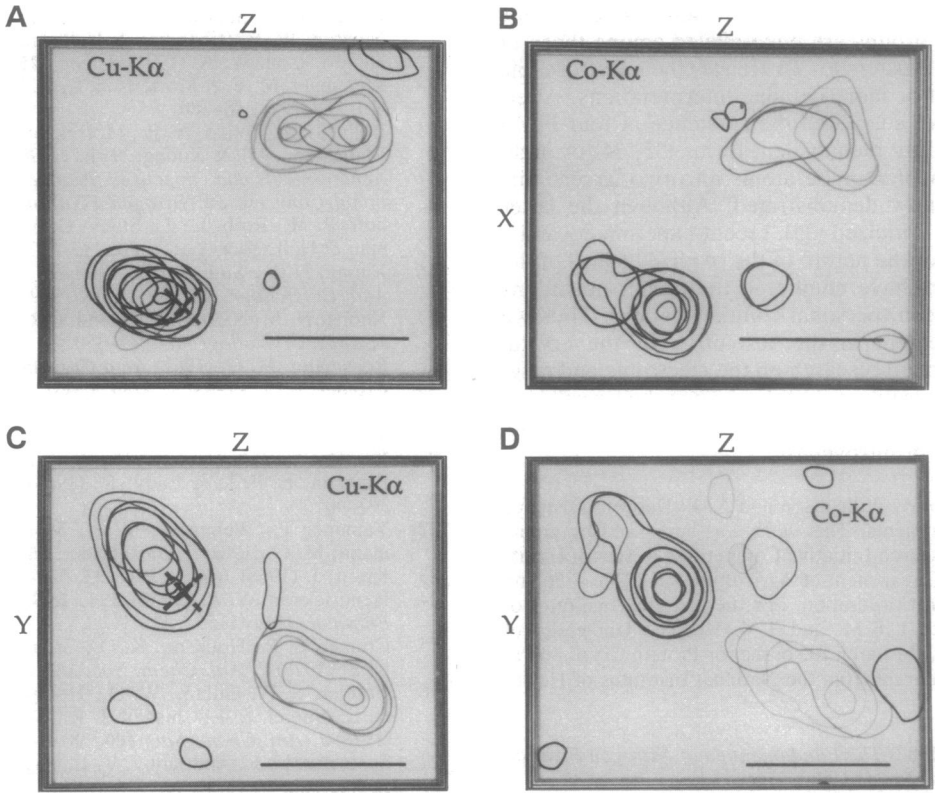

FIG. 2. MIR-phased Bijvoet difference electron density maps based on Cu-Kα and Co-Kα anomalous diffraction data. (*A* and *C*) Orthogonal views of a 24 × 23 × 28 Å block of the Cu-Kα map which includes density for one FeMoco and one all-Fe cluster. (*B* and *D*) Corresponding views of the same block from the Co-Kα map. Both maps were calculated by using reflections with spacings between 20 and 5 Å and were averaged about the molecular twofold symmetry axis. In both maps, the lowest contour is at 15% of the maximum value of the map and the interval between contours is 25% of the maximum. The FeMoco density is located in the lower left of *A* and *B* and the upper left of *C* and *D*, whereas the density of the all-Fe cluster is in the upper right of *A* and *B* and the lower right of *C* and *D*. An × plotted in *A* and *C* marks the position of the maximum in *B* and *D*; the solid line at the lower right of each panel is 10 Å long.

surface. These maps also indicate that the all-Fe center is somewhat closer to the surface, but we are unable to state with confidence whether either cluster, as found in the crystalline MoFe protein, is directly accessible to the Fe protein in solution. In this regard, it is interesting that the center-to-center separation of 19 Å between FeMoco and the all-Fe cluster is commensurate with the 20-Å distance found in the crystal structure of the Fe protein (12) for the separation between its Fe_4S_4 cluster and a probable binding site for the terminal phosphate of ATP [cf. Smith and Eady (7)]. We should also note that the edge-to-edge distance between the paired FeMoco and all-Fe clusters, 14 Å, is well within the range for which intramolecular long-range electron transfer is possible (28).

With regard to the structure of FeMoco, the Cu-Kα Bijvoet difference density indicates that the metal–sulfur framework is not spherical but rather has a shape similar to a prolate ellipsoid with an axial ratio of approximately 1.5:1 and a longest dimension in the range of 8–10 Å. Furthermore, the Cu-Kα density is not obviously resolved into subclusters, and the Co-Kα density shows that the Mo atom is located along the major axis of the ellipsoid at the periphery of the framework. When the prominent synthetic and hypothetical models for FeMoco are tested against these observations, incompatibilities arise in all cases. For example, the peripheral location of the Mo atom is in conflict with many of the models in a variety of structural classes. In addition, structures that can be classified as double cubanes (10, 11)—i.e., those that consist of two distinct metal–sulfur cubes linked by single or multiple light atom bridges—also are at odds with the first two observations. Analogues in this class have distinct subclusters separated by center-to-center distances significantly larger than 5 Å, and hence they should produce a more elongated density envelope plus evidence of subclusters similar to that found for the all-Fe cluster. Models based on the $Fe_6S_6(L)_6^{n-}$ prismane core (11), including capped prismanes, satisfy the criterion of a peripheral Mo atom and also possess 3.8-Å Fe–Fe separations compatible with recent Fe K-edge extended x-ray absorption fine structure (EXAFS) data for FeMoco and MoFe protein (ref. 29; S. P. Cramer & J. Chen, personal communication). However, in general they are more spherical and much smaller in the largest dimension than the Cu-Kα density envelope.

With regard to the noncofactor Fe atoms, our results show that the ≈16 Fe atoms previously assigned to four Fe_4S_4 P-clusters actually are located in two large superclusters, each of which comprises approximately 8 Fe atoms and is constructed of two subclusters. Thus our results establish that MoFe protein binds a metal–sulfur group of a type not previously observed in the crystal structure of a protein. Although we are unable to specify the precise atomic structure of the supercluster, its density is consistent with subclusters that resemble Fe_4S_4 clusters and, in consideration of the apparent distance between them, it is possible that the subclusters are covalently linked by bridging atom(s) or group(s).

The prior assignment of noncofactor Fe atoms to Fe_4S_4 P-clusters arose from interpretation of Mössbauer and EPR data (30) in the context of the properties of known FeS clusters. Subsequent cluster extrusion studies (31) and redox titrations (32) are consistent with the major features of this interpretation, although the latter identified three P-clusters and one cluster of a distinct type. It should be noted, however, that the original as well as subsequent Mössbauer

and EPR studies emphasize that the magnetic and electronic properties of these groups are unparalleled among those of protein-bound FeS clusters (5–7). Hence, the spectroscopic data allow different or more detailed interpretations. Alternative analyses have suggested the existence of four Fe_4S_4 clusters in two slightly inequivalent forms (33, 34) or organization of the noncofactor Fe atoms into two larger units (34), as we have now demonstrated. Although the latter model was initially criticized (35), recent experiments and a new interpretation of the nature of the oxidized states of the noncofactor clusters have countered the earlier objections (W. H. Orme-Johnson, personal communication). Thus we hope that improvement in the resolution of the crystal structure and continued research on the electronic and magnetic properties of this unusual "8-Fe" supercluster will lead to a synthesis of the available data and provide insight into its role in the function of nitrogenase.

J.T.B. is grateful to M. Williamson and X.-P. Dai for assistance with diffraction experiments. This work was supported by grants from the National Research Initiative Competitive Research Grants Program of the U.S. Department of Agriculture (89-37120-4786 and 91-37305-6662), Exxon Corporation, and the National Institutes of Health (GM 40067, to L.E.M. and T.V.M.). The University of California, San Diego, Research Resource for Protein Crystallography is supported by a grant from the National Institutes of Health (RR 01644).

1. Postgate, J. R. (1982) *The Fundamentals of Nitrogen Fixation* (Cambridge Univ. Press, Cambridge, U.K.).
2. Burris, R. H. (1991) *J. Biol. Chem.* **266,** 9339–9342.
3. Bishop, P. E., Jarlenski, M. L. & Hetheringon, D. R. (1980) *Proc. Natl. Acad. Sci. USA* **77,** 7342–7346.
4. Eady, R. R. (1991) *Adv. Inorg. Chem.* **36,** 77–102.
5. Orme-Johnson, W. H. (1985) *Annu. Rev. Biophys. Biophys. Chem.* **14,** 419–459.
6. Stiefel, E. I., Thomann, H., Jin, H., Bare, R. E., Morgan, T. V., Burgmayer, S. J. N. & Coyle, C. L. (1988) in *Metal Clusters in Proteins*, ed. Que, L., Jr. (Am. Chem. Soc., Washington), pp. 372–389.
7. Smith, B. E. & Eady, R. R. (1992) *Eur. J. Biochem.* **205,** 1–15.
8. Seefeldt, L. C., Morgan, T. V., Dean, D. R. & Mortenson, L. E. (1992) *J. Biol. Chem.* **267,** 6680–6688.
9. Burgess, B. K. (1990) *Chem. Rev.* **90,** 1377–1406.
10. Holm, R. H. & Simhon, E. D. (1985) *Metal Ions Biol.* **7,** 1–87.
11. Coucouvanis, D. (1991) *Acc. Chem. Res.* **24,** 1–8.
12. Georgiadis, M. M., Chakrabarti, P. & Rees, D. C. (1990) in *Nitrogen Fixation: Achievements and Objectives. Proceedings of the 8th International Congress on Nitrogen Fixation Research*, eds. Gresshoff, P. M., Roth, L. E., Stacy, G. & Newton, W. E. (Chapman & Hall, New York), pp. 111–116.
13. Hendrickson, W. A. (1991) *Science* **254,** 51–58.
14. Weininger, M. S. & Mortenson, L. E. (1982) *Proc. Natl. Acad. Sci. USA* **79,** 378–380.
15. Bolin, J. T., Ronco, A. E., Mortenson, L. E., Morgan, T. V., Williamson, M. & Xuong, N.-h. (1990) in *Nitrogen Fixation: Achievements and Objectives. Proceedings of the 8th International Congress on Nitrogen Fixation Research*, eds. Gresshoff, P. M., Roth, L. E., Stacy, G. & Newton, W. E. (Chapman & Hall, New York), pp. 117–122.
16. Xuong, N.-h., Sullivan, D., Nielsen, C. & Hamlin, R. (1985) *Acta Crystallogr. Sect. B* **41,** 267–269.
17. Xuong, N.-h., Nielsen, C., Hamlin, R. & Anderson, D. (1985) *J. Appl. Crystallogr.* **18,** 342–350.
18. Rossmann, M. G. (1961) *Acta Crystallogr.* **14,** 383–388.
19. Cromer, D. T. (1983) *J. Appl. Cryst.* **16,** 437.
20. Meyer, J. & Zaccai, G. (1981) *Biochem. Biophys. Res. Commun.* **98,** 43–50.
21. Voorduow, G., Haaker, H., van Breemen, J. F. C., van Bruggen, E. F. J. & Eady, R. (1983) *Eur. J. Biochem.* **136,** 397–401.
22. Yamane, T., Weininger, M. S., Mortenson, L. E. & Rossmann, M. G. (1982) *J. Biol. Chem.* **257,** 1221–1223.
23. Kraut, J. (1968) *J. Mol. Biol.* **35,** 511–512.
24. Hendrickson, W. A., Smith, J. L. & Sheriff, S. (1985) *Methods Enzymol.* **115,** 41–55.
25. Cramer, S. P., Hodgson, K. O., Gillum, W. O. & Mortenson, L. E. (1978) *J. Am. Chem. Soc.* **100,** 3398–3407.
26. Cramer, S. P., Gillum, W. O., Hodgson, K. O., Mortenson, L. E., Stiefel, E. I., Chisnell, J. R., Brill, W. J. & Shah, V. K. (1978) *J. Am. Chem. Soc.* **100,** 3814–3819.
27. Sosfenov, N. I., Andrianov, V. I., Vagin, A. A., Strokopytov, B. V., Vainshtein, B. K., Shilov, A. E., Gvozdev, R. I., Likhtenstein, G. I., Mitsova, I. Z. & Blazhchuk, I. S. (1986) *Sov. Phys. Dokl. (Engl. Transl.)* **31,** 933–935.
28. Fowler, B. E., Raphael, A. L. & Gray, H. B. (1990) *Prog. Inorg. Chem.* **38,** 259–322.
29. Arber, J. M., Flood, A. C., Garner, C. D., Gormal, C. A., Hasnain, S. S. & Smith, B. E. (1988) *Biochem. J.* **252,** 421–425.
30. Zimmerman, R., Münck, E., Brill, W. J., Shah, V. K., Henzl, M. T., Rawlings, J. & Orme-Johnson, W. H. (1978) *Biochim. Biophys. Acta* **537,** 185–207.
31. Kurtz, D. M., Jr., McMillan, R. S., Burgess, B. K., Mortenson, L. E. & Holm, R. H. (1979) *Proc. Natl. Acad. Sci. USA* **76,** 4986–4989.
32. Watt, G. D. & Wang, Z.-C. (1986) *Biochemistry* **25,** 5196–5202.
33. McLean, P. A., Papaefthymiou, V., Orme-Johnson, W. H. & Münck, E. (1987) *J. Biol. Chem.* **262,** 12900–12903.
34. Hagen, W. R., Wassink, H., Eady, R. R., Smith, B. E. & Haaker, H. (1987) *Eur. J. Biochem.* **169,** 457–465.
35. Lindahl, P. A., Papaefthymiou, V., Orme-Johnson, W. H. & Münck, E. (1988) *J. Biol. Chem.* **263,** 19412–19418.